

Quantum Electronics Letters

Re-Examining the Doping Effect on the Performance of Quantum Well Infrared Photodetectors

Mingrui Hao, Shuai Zhang, Yueheng Zhang, Wenzhong Shen, Harald Schneider, and Huichun Liu, *Fellow, IEEE*

Abstract—This paper investigates the dependence of background limited performance (BLIP) temperature of quantum well infrared photodetectors (QWIPs) on doping density. In contrast to the generally accepted optimal doping condition $E_F = k_B T_{BLIP}$, our theoretical prediction shows that lower doping densities should slightly increase the BLIP temperature T_{BLIP} taking into account the temperature dependence of the Fermi energy E_F , a factor neglected in the previous analyses. Numerical modeling results are used to reinterpret the reported T_{BLIP} measurements for a series of QWIPs of typical design for 9 μm peak wavelength with different doping values. In addition, based on the same general expression for the Fermi energy, the optimized sheet doping concentration to achieve maximum detectivity is given by $E_F = 1.37 \text{ } k_B T$, a revision to the previous $E_F = 2 \text{ } k_B T$ condition.

Index Terms—Quantum well infrared photodetectors (QWIPs), background limited performance (BLIP) temperature, doping density, detectivity.

I. INTRODUCTION

Quantum well infrared photodetectors (QWIPs) [1], [2] have been applied to focal plane arrays (FPA) for thermal imaging [3], [4] and high speed detectors [5], [6] in the mid- and long-wavelength infrared spectral range. To characterize the performance of QWIPs, systematic studies have been performed on the doping density dependence of the absorption coefficient α , quantum efficiency η , optical gain g , dark current I_{dark} , detectivity D^* and background limited performance (BLIP) temperature [1], [2], [7], [8]. The following statement is generally accepted: to achieve highest BLIP temperature (T_{BLIP}) and maximum D^* , the optimum Fermi energy E_F and hence the doping density is given by the conditions $E_F = k_B T_{BLIP}$ and $E_F = 2k_B T$, respectively [1], [2], [7], [8]. However, the approximation of T -independent E_F is no longer valid for elevated temperatures even in the cryogenic temperature regime. To analyze the T_{BLIP} dependence on E_F , we present here a numerical calculation using typical QWIP designs parameters and reinterpret the previous experimental

Manuscript received October 11, 2013; revised November 6, 2013; accepted November 7, 2013. Date of publication November 12, 2013; date of current version November 20, 2013. This work was supported in part by the National Major Basic Research under Projects 2011CB925603, in part by the Natural Science Foundation of China under Grants 91221201, 61234005, and 11074167, and in part by the 863 Program 2011AA010205.

M. R. Hao, S. Zhang, Y. H. Zhang, W. Z. Shen, and H. C. Liu are with the Department of Physics and Astronomy, Key Laboratory of Artificial Structures and Quantum Control (Ministry of Education), Shanghai Jiao Tong University, Shanghai 200240, China (e-mail: mrhao@sjtu.edu.cn; phybuff@sjtu.edu.cn; yuehzhang@sjtu.edu.cn; wzshen@sjtu.edu.cn; h.c.liu@sjtu.edu.cn).

H. Schneider is with the Institute of Ion-Beam Physics and Materials Research, Helmholtz-Zentrum Dresden-Rossendorf, Dresden D-01314, Germany and also with the Department of Physics and Astronomy, Key Laboratory of Artificial Structures and Quantum Control (Ministry of Education), Shanghai Jiao Tong University, Shanghai 200240, China (e-mail: h.schneider@hzdr.de).

Color versions of one or more of the figures in this letter are available online at <http://ieeexplore.ieee.org>.

Digital Object Identifier 10.1109/JQE.2013.2290535

results. The theoretical prediction does not support the existence of an “optimal doping” for maximum T_{BLIP} and implies that T_{BLIP} will increase slightly with decreasing doping density. The reported experimental results are consistent with our calculated T_{BLIP} values. In addition, based on the same general expression of the Fermi energy, we predict the optimum sheet doping concentration at $E_F = 1.37 \text{ } k_B T$ to achieve maximum detectivity.

II. ANALYSIS

The total current through a photodetector is composed of dark current I_{dark} and photocurrent I_{ph} . Both signal and background radiation can excite photocurrent and the latter is usually relatively high for infrared detection. The BLIP temperature T_{BLIP} is the characteristic temperature at which the background photocurrent equals the dark current. Under background limited performance, the intrinsic noise of the detector is negligible in comparison with the noise from the fluctuation of the background photon flux. The dark current of typical QWIP structures, described by the three-dimensional (3D) carrier drift model [2] accounting for the thermally excited carriers from the well and flowing above the barriers, is given by

$$I_{dark} = 2 \left(\frac{m_b^* k_B T}{2\pi \hbar^2} \right)^{\frac{3}{2}} \exp \left(-\frac{E_{act}}{k_B T} \right) e V_{drift}(F) A \quad (1)$$

where e is electron charge and A is detector area, \hbar is the reduced Planck constant, k_B is the Boltzmann constant, $V_{drift}(F)$ is the electron average drift velocity in the barrier region which depends on electric field F , m_b^* is the barrier effective mass, T is temperature, E_{act} is the thermal activation energy which equals the energy difference between the barrier height and the Fermi level in the well. Neglecting the bias field-induced barrier lowering effect, we have $E_{act} = V_b - E_F$. The background photocurrent $I_{ph,bg}$ is given by the standard expression

$$I_{ph,bg} = e A \eta \frac{\tau_{cap} V_{drift}(F)}{N L_p} \phi_{bg} \quad (2)$$

where η is the absorption quantum efficiency, Φ_{bg} is the photon number flux of background radiation, N is the number of quantum wells (QWs), τ_{cap} is the electron capture time into the well and L_p is the QW period width which equals the sum of the well width and the barrier width. Since the capture process is determined by LO phonon scattering, we use the approximation given in Ref. [9] as an estimate for τ_{cap} .

Using the 3D carrier drift dark current model, T_{BLIP} is obtained from the following relationship [2] by equating (1) and (2),

$$\eta^{(1)} \tau_{cap} \phi_{bg} = 2 L_p \left(\frac{m_b^* k_B T}{2\pi \hbar^2} \right)^{\frac{3}{2}} \exp \left(\frac{E_F}{k_B T} - \frac{hc}{\lambda k_B T} \right) \quad (3)$$

where c is the light speed, h is the Planck constant, $\eta^{(1)}$ is the absorption quantum efficiency for one well and λ is the cutoff wavelength of detector. E_F depends on both the temperature and the 2D carrier concentration [8], [10] in the well N_{2D}

$$N_{2D} = \frac{m}{\pi \hbar^2} k_B T \ln \left[1 + \exp \left(\frac{E_F}{k_B T} \right) \right] \quad (4)$$

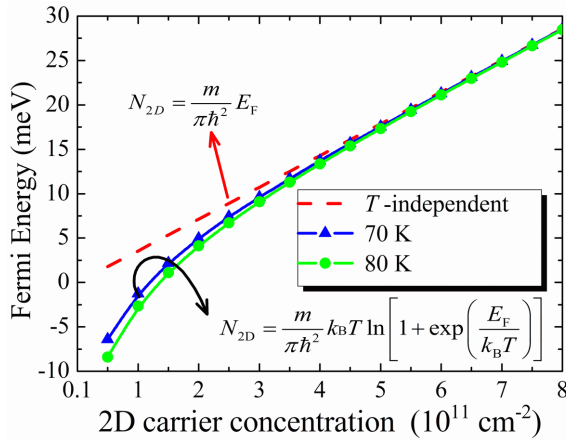


Fig. 1. Different approaches for calculating the Fermi energy as a function of the 2D carrier concentration in the QW. The E_F ignoring temperature effect is plotted using a dashed line, while the E_F values which account for temperature effect are plotted for 70 K (triangles) and 80 K (circles), respectively. The Fermi energy value is referenced to the ground state energy in the well.

where m is the QW effective mass. E_F is referenced to the ground state energy E_1 . If $E_F/k_B T \gg 1$ is valid, we get the approximation

$$E_F = \frac{\pi \hbar^2}{m} N_{2D} \quad (5)$$

in which the temperature variation is ignored for simplicity. $\eta^{(1)}$ is proportional to N_{2D} taking into account the impact of the spectral broadening [7], [10], $\eta^{(1)} = \kappa N_{2D}/\delta E$, where κ represents the proportionality coefficient which is related to QW structure parameters, δE is the half width at half maximum of the absorption lineshape. Based on this approach, the absorption for one well and thus the Fermi energy are proportional to N_{2D} , which thus yields $\eta^{(1)} \sim E_F$.

In previous analyses, combining Eq. (3) with Eq. (5), T_{BLIP} is determined by solving the following transcendental equation

$$\frac{E_F}{k_B T} \exp\left(-\frac{E_F}{k_B T}\right) = \frac{(\delta E)L_P(m_b^*)^{\frac{3}{2}}}{\tau_{cap}\phi_{bg}m\kappa} \left(\frac{k_B T}{2\pi\hbar^2}\right)^{\frac{1}{2}} \exp\left(-\frac{hc}{\lambda k_B T}\right) \quad (6)$$

One can adjust the ratio $E_F/k_B T$ to maximize the left-hand side of Eq. (6), so that the trend of T_{BLIP} is related to a function of the ratio $E_F/k_B T$. Under this approximation, the ratio $E_F/k_B T$ can be used as an adjustable parameter, T_{BLIP} reaches its maximum value at $E_F/k_B T = 1$. From the above discussion the generally accepted conclusion is that $E_F = k_B T_{BLIP}$ is the optimal doping for maximum T_{BLIP} .

The optimal doping is characterized in terms of the ratio $E_F/k_B T$, based on the assumption that E_F is proportional to N_{2D} for simplicity. However, is the assumption of temperature independent E_F a good approximation for realistic QWIPs? Considering n-doped GaAs/Al_xGa_{1-x}As quantum well structures, Fig. 1 compares the temperature dependent and independent Fermi energy approaches as a function of the 2D carrier concentration. The E_F which ignored the temperature effect is plotted using a dashed line, while the E_F values obtained from Eq. (4), which account for the temperature effect are plotted for 70 K (triangles) and 80 K (circles), respectively. The Fermi energy value is referenced to the ground state energy in the well. As seen in Fig. 1, at carrier concentrations below $N_{2D} < 4 \times 10^{11} \text{ cm}^{-2}$, E_F values become temperature dependent and show significant nonlinear dependence on N_{2D} . The nonlinearity is even more pronounced for decreasing carrier concentra-

tion. Only in the regime $N_{2D} > 5 \times 10^{11} \text{ cm}^{-2}$, the difference between the E_F values raised by the T -independent model can be neglected. The approximation of T -independent E_F is not satisfied for realistic carrier concentrations in cryogenic temperature regime. Therefore, the previous characterization on T -independent E_F cannot accurately reflect the relationship between the T_{BLIP} and the carrier concentration.

Assuming a complete ionization of the donors, the nonlinear dependence of E_F on doping density cannot be ignored in the operation temperature regime of QWIPs. In order to derive a more general and precise T_{BLIP} dependence involving temperature effects on E_F , Eq. (6) should be replaced by

$$\begin{aligned} \ln\left[1 + \exp\left(\frac{E_F}{k_B T}\right)\right] \exp\left(-\frac{E_F}{k_B T}\right) \\ = \frac{(\delta E)L_P(m_b^*)^{\frac{3}{2}}}{\tau_{cap}\phi_{bg}m\kappa} \left(\frac{k_B T}{2\pi\hbar^2}\right)^{\frac{1}{2}} \exp\left(-\frac{hc}{\lambda k_B T}\right) \quad (7) \end{aligned}$$

in which the right-hand side is the same. The trend of T_{BLIP} is determined by the competition between photocurrent and dark current. The ratio $E_F/k_B T$ is associated with the doping level, larger positive ratio represents higher doping density, while negative ratio corresponds to relatively low doping such that the Fermi energy is below the ground state. The left-hand side of Eq. (7) approaches $1 - 0.5 \times \exp(E_F/k_B T)$ in the region of “low” $E_F/k_B T$, i.e., $E_F/k_B T \ll -1$. This implies that T_{BLIP} will slightly increase with decreasing carrier concentration. However, reducing the doping level to achieve higher T_{BLIP} leads to reduced absorption, which is undesirable for the detector performance.

III. RESULTS AND DISCUSSION

We present a numerical calculation to reinterpret the previous experimental results. For a typical QWIP, accounting for the carriers distributed above the barrier, E_F is determined by the following

$$N_{dope} = \int_0^\infty \rho_{2D}(\varepsilon) f(\varepsilon) d\varepsilon + L_p \int_{V_b - E_1}^\infty \rho_{3D}(\varepsilon) f(\varepsilon) d\varepsilon \quad (8)$$

where N_{dope} is the equivalent sheet doping density in the well, V_b is the barrier height, $f(\varepsilon)$ is the Fermi-Dirac distribution function, $\rho_{2D} = m/(\pi\hbar^2)$ is the 2D density of states in the well and ρ_{3D} is the 3D density of states above the barrier. For the Fermi energy calculation, we used the QWIP parameters taken from Ref. [8]. This QWIP series designed for about $9.5 \mu\text{m}$ cutoff wavelength had a measured peak wavelength of about $8.9 \mu\text{m}$. The samples had nominally identical QW parameters but different doping densities in the well with 2D equivalent doping densities ranging from 2×10^{11} to $8 \times 10^{11} \text{ cm}^{-2}$. The calculation shows that the 3D states carriers make up very little proportion in total carriers in cryogenic temperature regime, so that Eq. (4) should be a good approximation.

The T -dependent E_F are calculated from Eq. (7). Assuming N_{dope} ranges from $5 \times 10^{10} \text{ cm}^{-2}$ to $1 \times 10^{12} \text{ cm}^{-2}$, for $9 \mu\text{m}$ peak wavelength QWIPs with $\pi/2$ FOV and for 300 K background radiation, the numerically modeled T_{BLIP} are shown as a function of the ratio $E_F/k_B T$ and the sheet doping density in Figs. 2(a) and 2(b), respectively. T_{BLIP} values as obtained using a T -independent E_F are shown in Fig. 2(b) for comparison. The T_{BLIP} values predicted by the two models differ by 1.2 K at $2 \times 10^{11} \text{ cm}^{-2}$ and by as much as 2.7 K at $1 \times 10^{11} \text{ cm}^{-2}$. The experimental T_{BLIP} results from Ref. [8] are also plotted in Figs. 2(a) and 2(b) as a function of the corresponding ratio $E_F/k_B T$ and doping density, respectively. The theoretical values of T_{BLIP} using T -dependent E_F are in good agreement with the experimental results. Both the theoretical modeling with T -dependent E_F and the measurements show that T_{BLIP} will increase

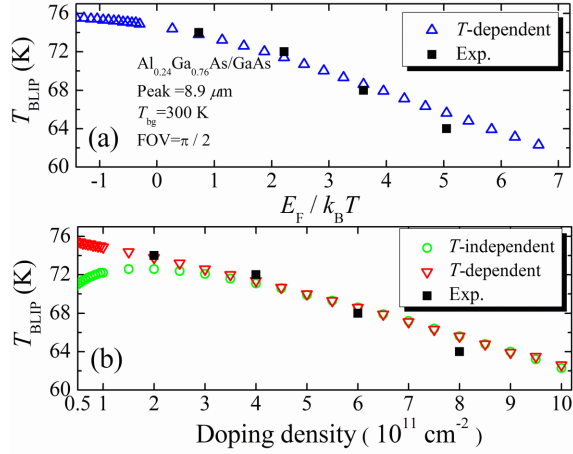


Fig. 2. Calculated T_{BLIP} for $9 \mu\text{m}$ QWIPs as a function of (a) ratio $E_F/k_B T$ using T -dependent E_F (up triangles) and (b) sheet doping density using T -independent E_F (circles) and T -dependent E_F (down triangles), with $\pi/2$ FOV and for 300 K background radiation. The measured T_{BLIP} (solid squares) are taken from Ref. [8].

with decreasing doping. The present theory contradicts the previous prediction $E_F/k_B T = 1$ (in this case equivalent doping density $2.3 \times 10^{11} \text{ cm}^{-2}$) for the optimal condition to achieve the highest T_{BLIP} .

In addition, we extend the analysis to detectivity D^* as a function of the doping density. D^* is defined as the signal to noise ratio normalized by the incident power, detector area A and electrical bandwidth Δf of the measurement, i.e., $D^* = R(A\Delta f)^{1/2}/i_{\text{noise}}$, where R is the responsivity and i_{noise} is the current noise of the detector. Using the expressions $i_{\text{noise}} = (4eI_{\text{dark}}g\Delta f)^{1/2}$ and $R = e(\lambda/hc)\eta g$, where g is the gain, D^* is written as

$$D^* = \frac{\lambda\eta(1)}{2hc} \left(\frac{\tau_{\text{cap}}N}{L_p} \right)^{\frac{1}{2}} \left[2 \left(\frac{m_b^* k_B T}{2\pi\hbar^2} \right)^{\frac{3}{2}} \exp \left(-\frac{E_{\text{act}}}{k_B T} \right) \right]^{-\frac{1}{2}} \quad (9)$$

It is proportional to

$$D^* \propto \ln \left[1 + \exp \left(\frac{E_F}{k_B T} \right) \right] \exp \left(-\frac{E_F}{2k_B T} \right) \quad (10)$$

which is consistent with the result of Gunapala *et al* [7]. As a consequence, the numerical calculation predicts that the maximum D^* exists at $E_F/k_B T = \ln \{ \exp[W(-2/e^2)+2]-1 \} \approx 1.37$, where W denotes Lambert W function [11].

In addition to the doping level, the doping profile also has impact on the device performance [12]–[14]. A different doping profile affects the ionized impurity scattering and involves an electrostatic reconfiguration. Solving the self-consistent Poisson equation, we can get a more accurate energy band profile. However, the condition $E_F = 1.37 k_B T$ should still remain valid.

The theoretically predicted dependence of D^* on the ratio $E_F/k_B T$ for the $9 \mu\text{m}$ QWIPs at 80 and 85 K is shown in Fig. 3. Compared with the experimental results [8], both imply that there is indeed an optimal doping to achieve the highest D^* if dark current noise dominates. Our prediction $E_F/k_B T = 1.37$ is somewhat different from the generally accepted relation $E_F/k_B T = 2$. The amount of peak D^* is expected to decrease by 2.8% when the ratio $E_F/k_B T$ changes from 1.37 to 2. Using the new optimal condition and Eq. (4), to achieve the maximum D^* , the desired sheet doping concentration is $N_{\text{dope}} = 3.84 \times 10^9 (\text{cm}^{-2}\text{K}^{-1}) \times T(\text{K})$ for the GaAs/ $\text{Al}_x\text{Ga}_{1-x}\text{As}$ system, where T is the operating temperature of QWIPs.

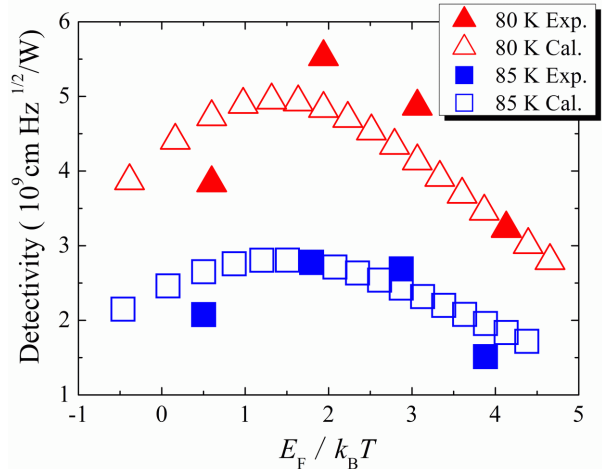


Fig. 3. Theoretically predicted detectivity dependence of the ratio $E_F/k_B T$ for a typical $9 \mu\text{m}$ QWIP at 80 K (empty triangles) and 85 K (empty squares), respectively. The experimental data at 80 K (solid triangles) and 85 K (solid squares) taken from Ref. [8] are reproduced.

The condition for optimum D^* derived here is relevant for QWIP single detectors and FPAs which are limited by the noise arising from dark (i.e. thermally induced) conductivity. This limitation is a practical issue since low operation temperature usually has the penalty of increased power consumption and reduced lifetime of the cryo-cooler. Optimizing this “dark-limited” D^* is crucial in particular for long detection wavelengths where the cooling system has to operate close to its limits. In order to achieve good noise equivalent temperature difference (NETD), devices with high quantum efficiency are generally desirable, in particular if short integration times are needed. If high quantum efficiency is considered more important than high T_{BLIP} , then the doping density should be increased [15].

IV. CONCLUSION

In conclusion, by analyzing the influence of doping concentration on background limited performance temperature of QWIPs, our theory prediction shows that T_{BLIP} increases monotonously with decreasing carrier density, which is inconsistent with the generally accepted condition $E_F = k_B T_{\text{BLIP}}$ for maximum T_{BLIP} . We also find the optimal sheet concentration for maximum detectivity at $E_F = 1.37 k_B T$.

REFERENCES

- [1] B. F. Levine, “Quantum-well infrared photodetectors,” *J. Appl. Phys.*, vol. 74, no. 8, pp. R1–R81, Oct. 1993.
- [2] H. Schneider and H. C. Liu, *Quantum Well Infrared Photodetectors—Physics and Applications* (Springer Series in Optical Sciences), vol. 126. Berlin, Germany: Springer-Verlag, 2007, pp. 45–72.
- [3] S. D. Gunapala, S. V. Bandara, J. K. Liu, J. M. Mumolo, D. Z. Ting, C. J. Hill, *et al.*, “Demonstration of megapixel dual-band QWIP focal plane array,” *IEEE J. Quantum Electron.*, vol. 46, no. 2, pp. 285–293, Feb. 2010.
- [4] K. K. Choi, D. P. Forrai, D. W. Endres, and J. Sun, “Corrugated quantum-well infrared photodetector focal plane arrays,” *IEEE J. Quantum Electron.*, vol. 45, no. 10, pp. 1255–1264, Oct. 2009.
- [5] R. Paiella, F. Capasso, C. Gmachl, D. L. Sivco, J. N. Baillargeon, A. L. Hutchinson, *et al.*, “Self-mode-locking of semiconductor lasers with giant ultrafast optical nonlinearities,” *Science*, vol. 290, no. 5497, pp. 1739–1742, Dec. 2000.
- [6] A. Hugi, G. Villares, S. Blaser, H. C. Liu, and J. Faist, “Mid-infrared frequency comb based on a quantum cascade laser,” *Nature*, vol. 492, pp. 229–233, Dec. 2012.

- [7] S. D. Gunapala, B. F. Levine, L. Pfeiffer, and K. West, "Dependence of the performance of GaAs/AlGaAs quantum well infrared photodetectors on doping and bias," *J. Appl. Phys.*, vol. 69, no. 9, pp. 6517–6520, May 1991.
- [8] Y. Yang, H. C. Liu, W. Z. Shen, N. Li, W. Lu, Z. R. Wasilewski, *et al.*, "Optimal doping density for quantum-well infrared photodetector performance," *IEEE J. Quantum Electron.*, vol. 45, no. 6, pp. 623–628, Jun. 2009.
- [9] J. Y. Andersson, "Dark current mechanisms and conditions of background radiation limitation of n-doped AlGaAs/GaAs quantum-well infrared detectors," *J. Appl. Phys.*, vol. 78, no. 10, pp. 6298–6304, Nov. 1995.
- [10] H. C. Liu, "Dependence of absorption spectrum and responsivity on the upper state position in quantum well intersubband photodetectors," *J. Appl. Phys.*, vol. 73, no. 6, pp. 3062–3067, Mar. 1993.
- [11] R. M. Corless, G. H. Gonnet, D. E. G. Hare, D. J. Jeffrey, and D. E. Kunth, "On the Lambert W function," *Adv. Comput. Math.*, vol. 5, no. 1, pp. 329–359, Feb. 1996.
- [12] H. C. Liu, Z. R. Wasilewski, and M. Buchanan, "Segregation of Si delta doping in GaAs-AlGaAs quantum wells and the cause of the asymmetry in the current-voltage characteristics of intersubband infrared detectors," *Appl. Phys. Lett.*, vol. 63, no. 6, pp. 761–763, Aug. 1993.
- [13] E. B. Dupont, D. Delacourt, D. Papillon, J. P. Schnell, and M. Papchon, "Influence of ionized impurities on the linewidth of intersubband transitions in GaAs/GaAlAs quantum wells," *Appl. Phys. Lett.*, vol. 60, no. 17, pp. 2121–2122, Apr. 1992.
- [14] E. Luan, A. Guzman, J. L. Sanchez-Rojas, J. M. Sanchez, and E. Munoz, "GaAs-based modulation-doped quantum-well infrared photodetectors for single- and two-color detection in 3–5 μm ," *IEEE J. Sel. Topics Quantum Electron.*, vol. 8, no. 5, pp. 992–997, Sep./Oct. 2002.
- [15] H. Schneider, J. Fleissner, R. Rehm, M. Walther, W. Pletschen, P. Koidl, *et al.*, "High-resolution QWIP FPAs for the 8–12 μm and 3–5 μm regimes," *Proc. SPIE*, vol. 4820, pp. 297–305, Jan. 2003.